DEVELOPMENT OF A QUANTITATIVE FLAW CHARACTERIZATION MODULE - A STATUS REPORT*

George J. Gruber, Gary J. Hendrix and
Theodore A. Mueller

Southwest Research Institute

ABSTRACT

Ultrasonic waves returning from an internal bulk flaw to a wideband transducer contain information on several characteristics of this flaw. Measurements made with waves of different mode, dominant frequency, incidence angle, beamwidth, etc. are, therefore, necessary to solve the inverse problem for flaw composition, size, and orientation in an unambiguous manner.

The plan for the development of a reliable and accurate volumetric-flaw characterization module encompasses three basic elements: a transducer selection protocol, a deconvolution algorithm, and the Born as well as the Franz-Gruber (satellite pulse) models for the interaction of weakly and strongly scattering internal bulk flaws, respectively. The flaw-diameter estimates obtained by applying the Born Inversion Technique (BIT) and the Satellite-Pulse Observation Technique (SPOT), based on the above models, to the results of ultrasonic backscattering experiments are compared in this paper with the nominal effective diameters of five spherical voids in a titanium-alloy specimen tested under blind conditions.

*This work is supported by the U.S. Department of the Air Force under Contract F33615-81-C-5066, "Exploratory Development for a High Reliability Quantitative Flaw Characterization Module."

INTRODUCTION

Life-management technology now being developed for the Air Force under the name "retirement for cause" requires reliable and accurate ultrasonic techniques for characterizing internal bulk flaws in titanium- and nickel-based alloy disk materials. One objective of the Quantitative Nondestructive Evaluation (NDE) program, established in the mid-1970s, was to develop inverse-scattering algorithms as well as pattern-recognition methods for the characterization of flaws as to type, size, and orientation (1). The sizing techniques developed on the basis of the complementing Born and Franz-Gruber (satellite pulse) models for the interaction of ultrasound with internal bulk flaws are ready for performance evaluation.

Figure 1 shows a flow diagram of the program established to qualify the Born Inversion Technique (BIT) for sizing voids and inclusions in typical aircraft turbine-engine parts. An opportunity also existed to apply the Satellite-Pulse Observation Technique (SPOT) to the five voids tested to date under blind conditions to ascertain if the flaw size were such that the BIT can be used to estimate the void diameter with acceptable inaccuracy. The accuracies of the BIT and the SPOT were determined by comparing the average of several throughwall-dimension estimates with the nominal diameters of the spherical voids in a titanium-alloy specimen.

ULTRASOUND-FLAW INTERACTION MODELS

The sketches in Figure 2 reveal in the dimensionless ka-parameter* domain the differences and similarities between the transfer function H(ka) of a weakly scattering, inclusion-like flaw (Born model) and that of a strongly scattering, void-like flaw (Franz model). The principles of the BIT and the SPOT for volumetric-flaw sizing can best be formulated in the time domain as presented below.

Born Model for Spherical Inclusions

The basic assumption of the Born model is that the change in material properties between the flaw and its host is negligibly small. The impulse response h(t) of a weakly scattering spherical inclusion consists of two pulses: a front-surface echo

*$k=2\pi f/c$ where f is the transducer center frequency and c is the longitudinal-wave velocity of the host material, and a is the radius of the spherical scatterer (= d/2).

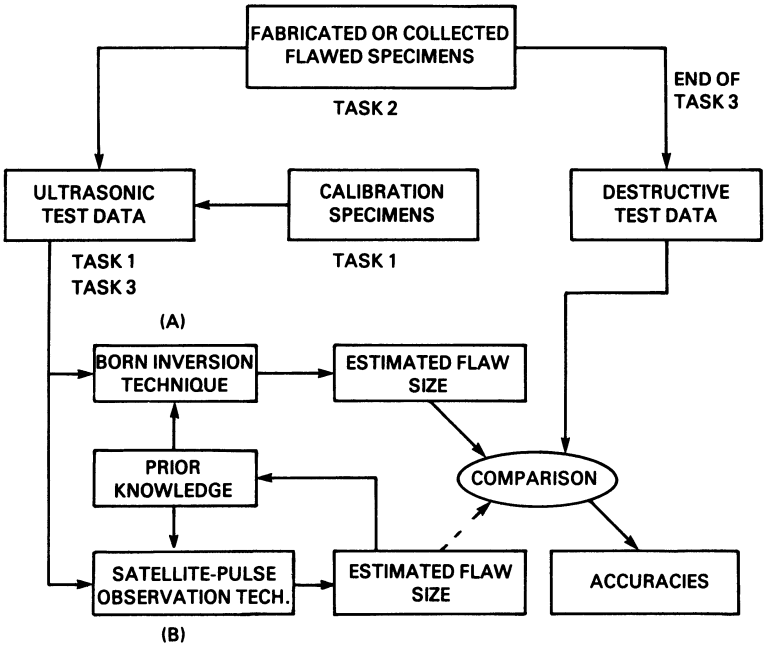

Fig. 1. Flow Diagram of Effort to Qualify the Born Inversion Technique for the Characterization of Voids and Inclusions.

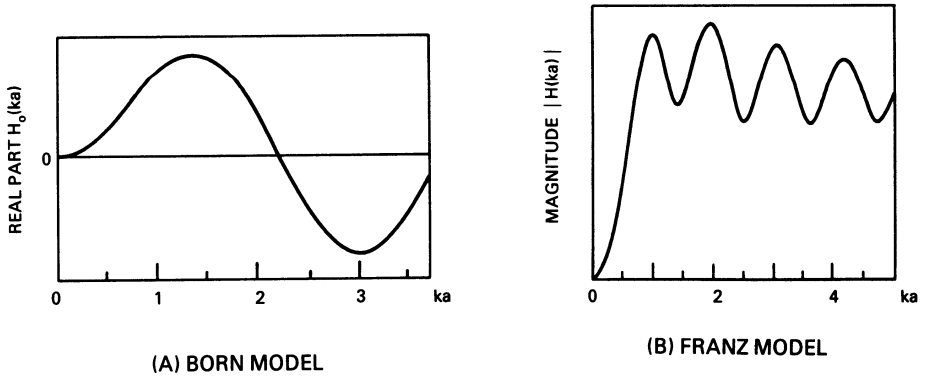

Fig. 2. Variation of Backscattered Signal Amplitude with "ka" for Model Scatterers of Radius "a". (A) Spherical Inclusion (after Reference 2), (B) Spherical Void (after Reference 3).

(F pulse) and a comparable back-surface echo (B pulse). In Figure 3(a), the F and B pulses are placed symmetrically about the center of the flaw marked by the origin of the time axis. The delay time between the F and B pulses Δ_b is given by 2d/c. The one-dimensional BIT requires long-wavelength (ka<1) measurements to estimate the location of the center of the flaw (2). Actually, to avoid significant underestimation as well as overestimation of flaw size,* the low-ka cutoff must be less than 0.5 and the high-ka cutoff must be greater than 2.0, respectively (3). Before applying the BIT to the results of longitudinal-wave backscattering measurements, it is, therefore, necessary to assure that both the center frequency and the bandwidth of the employed transducer are "proper" for the flaw in question.

One way to solve the transducer-selection problem is to acquire backscattered waveforms from a given flaw with wideband transducers having successively lower center frequencies (3). To understand how the center frequency influences the Born-diameter estimate d_b, it is helpful to consider the magnitude spectrum of a spherical void** shown in Figure 2(b). Below some wavenumber (ka<0.5), there will be no additional peaks in the flaw's transfer function $|H(ka)|$, but only a k^2 dependence. The transducer whose response function $|W(f)|$ is centered around ka=1[=(0.5 x 2)$^{\frac{1}{2}}$] is the proper one to use. It is, therefore, necessary to resort to the use of three or more transducers if the range of flaw sizes is expected to be wide (e.g., flaw diameters ranging from 250 to 1,300 μm as in the current program).

The input to the Born inverse-scattering algorithm consists of the real part of the deconvolved flaw spectrum $H_o(k)$ obtained with an appropriate longitudinal-wave transducer. The experimental protocol for obtaining the flaw waveforms y(t) and reference waveforms w(t) was developed under the guidance of Ames Laboratory (4). A deconvolution algorithm of the Wiener-filter type was derived to minimize the effects of transducer and material properties on d_b. Deconvolution is accomplished by obtaining w(t) from the specimen's back surface, fourier transforming y(t) and w(t), and forming the division

$$H(f) = \frac{Y(f)\, W^*(f)}{|W(f)|^2 + Q^2} \qquad (1)$$

*Sizing errors greater than 20 percent are considered to be significant.

**In this analysis, the void is considered as a special case of an inclusion (i.e., a strongly scattering inclusion).

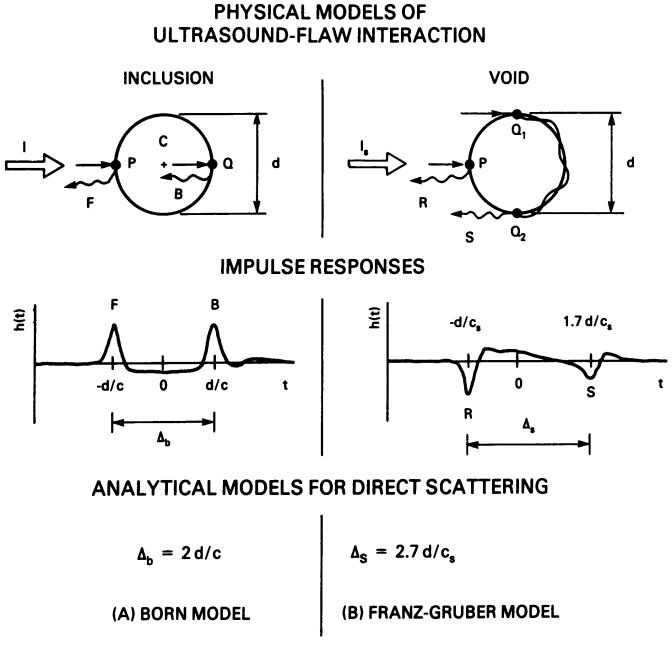

Fig. 3. Impulse Responses of Model Scatterers (after Reference 2). (A) Spherical Inclusion, (B) Spherical Void in Titanium.

Here, Y(f) is the flaw spectrum, W(f) is the reference spectrum, the asterisk denotes complex conjugate, and Q^2 represents the average spectral power density of the background interference.

Accurate estimation of the flaw center's location relative to the time coordinate system from low-frequency ($ka<0.5$) deconvolved data is essential to the success of the BIT. Several methods have been proposed to make the center of the flaw correspond to the origin of time, including flattening the characteristic function J(r) at range r=0 (3), flattening the phase spectrum at low frequencies (3), and maximizing the cross-sectional area function (2). In the Ames Laboratory transferred zero-of-time algorithm, the origin of time is chosen at the maximal cross-sectional area.

The effective flaw diameter* (Born diameter) can be derived from the flaw's characteristic function that is related to the measurable transfer function by the inversion formula

$$J(r) = \text{constant} \int_{k_{min}}^{k_{max}} H_o(k) \frac{\sin 2kr}{2kr} dk \qquad (2)$$

The values of k_{min} and k_{max} are governed, respectively, by the lowest and highest usable frequencies in the transducer response function. It is understood that the entire transfer function in Eq. (2) is to be derived from a single y(t) and w(t) obtained with the same transducer.

The BIT yields an estimate of the distance from the flaw's center of mass [point C in Figure 3(a)] to the front-surface tangent plane (half the Born diameter). Several methods have been proposed to obtain the Born diameter from the characteristic function (3), including dividing the area under the characteristic function by its peak value and multiplying the result by 2, i.e.,

$$d_b = 2 \frac{\text{Area under } J(r)}{\text{Peak Value of } J(r)} \qquad (3)$$

Franz-Gruber Model for Spherical Voids

Another way to solve the transducer-selection problem of the BIT for void-like flaws is to insonify the flaw in question with short, high-frequency shear waves and relate the separation of the backscattered satellite pulse [S in Figure 3(b)] from the reflected pulse [R in Figure 3(b)] to its "approximate dimension" (5).** Freedman (6) assumed the waveform received from a void-like flaw of convex shape to be composed of several discrete pulses, each identical to the transmitted pulse. The first pulse is produced by the specular reflection of the incident wave at the point on the flaw surface nearest to the source of ultrasound [i.e., at point P in Figure 3(b)]. Additional (satellite) pulses are formed whenever there is a discontinuity in solid angle subtended at the transducer by parts of the flaw within range r or in its nth derivative with respect to range. The magnitude of each satellite pulse decreases with increasing ka.

*Effective flaw diameter is the dimension of a volumetric flaw in the direction of the incident longitudinal wave [I in Figure 3(a)].
**The amplitude-drop technique, featuring a focused transducer, was not considered a viable "second method for rough flaw characterization."

Franz (7) termed the waves producing the extra pulses appearing in the ultrasonic signature of a spherical void in a metal "creeping waves." The first pair of Franz waves arrive at the transducer simultaneously after having traveled ("crept") once around the back surface of the void in opposite directions. For clarity, only the clockwise creeping wave is shown by the wavy line from Q_1 to Q_2 in Figure 3(b). The mode-converted (surface) waves produced by the incident bulk wave at the void's shadow boundaries circumvent it a number of times until they disappear into the background of irrelevant sources since their energy is continuously depleted by tangential radiation (8). Each time the clockwise creeping wave reaches point Q_2, a tangentially scattered wave (S wave) is launched in the desired direction to be received by the shear-wave transducer. The separation between the R pulse and its nearest satellite (S pulse) is a linear function of the void diameter as expressed by the relationship

$$\Delta_s = \left(\frac{1}{c_s} + \frac{\pi}{2v}\right) d \tag{4}$$

where c_s is the shear-wave velocity and v is the Rayleigh-wave velocity of the host material. Using 6.10 and 3.12 mm/μs, respectively, for the longitudinal- and shear-wave velocites of Ti-6-4 and $v = 0.93c_s$, Eq. (4) becomes

$$\Delta_s = 2.7d/c_s \tag{5}$$

The void diameter is estimated from the results of high-frequency shear-wave measurements by the equation

$$d_s = 1.15\ \Delta_s \tag{6}$$

It can be shown (9) that 10-MHz creeping waves produced on the surface of a 800-μm diameter void in Ti-6-4 by incident longitudinal waves travel with a velocity that is 92 percent of c. High-frequency longitudinal-wave measurements provide less accurate SPOT-diameter estimates than shear-wave measurements according to the equation*

$$d_\ell = 2.25\Delta_\ell \tag{7}$$

*Note that the constants in Eqs. (6) and (7) are related to each other as the two bulk-wave velocities (c_s and c).

ALGORITHM PERFORMANCE EVALUATION

The objective of the first set of blind tests was to determine the validity of the candidate transducer-selection methods to be incorporated into the quantitative flaw-characterization procedures. Longitudinal-wave data for Born inversion were acquired for each test flaw with four transducers whose center frequencies were in the 1.9 to 10.8 MHz range to prevent an inadvertent error in the selection of a longitudinal-wave transducer based on the initial high-frequency shear-wave measurements. This frequency range was judged to be sufficiently wide for the first five test flaws that were known to be spherical voids with diameters in the 250 to 1,300 m range. These flaws were placed into a diffusion-bonded Ti-6-4 plate specimen by Pratt & Whitney Aircraft Group (10).

Shear-Wave Measurements

Representative waveforms $y_s(t)$ received from the five test flaws by 7-MHz shear-wave transducers are shown in Figure 4 against the background of a reference waveform $w_s(t)$ obtained from a 2-mm diameter side-drilled hole. Except for the smallest void (Flaw 01), the satellite pulses trailing the reflected pulses could be readily identified by the "blinded" ultrasonic examiner. The examiner converted the doublet separations Δ_s into SPOT-diameter estimates d_s using Eq. (6). These estimates, listed in Table 1, appear to agree well with the nominal flaw diameters (11).

Longitudinal-Wave Measurements

While waveforms were acquired for each flaw with four broadband, immersion-type, Panametric transducers (center frequencies of 1.9, 4.1, 9.2 and 10.8 MHz) transmitting 45-degree longitudinal waves into the test specimen, only those flaw data were Born inverted that were obtained with transducer(s) judged to be the best compromise for a flaw initially tested with shear waves. The center frequency for the most appropriate longitudinal-wave transducer (optimum frequency f_o) is determined from the average result of shear-wave measurements by the equation

$$f_o = 1{,}950/d_s \qquad (8)$$

where f_o is in MHz and d_s is in μm.

Table 2 contains the optimum frequencies calculated for the five test flaws. The center frequencies of the most appropriate available longitudinal-wave transducers are listed in the last column. Only for one void (Flaw 02) did the optimum frequency coincide with the center frequency of one of the available

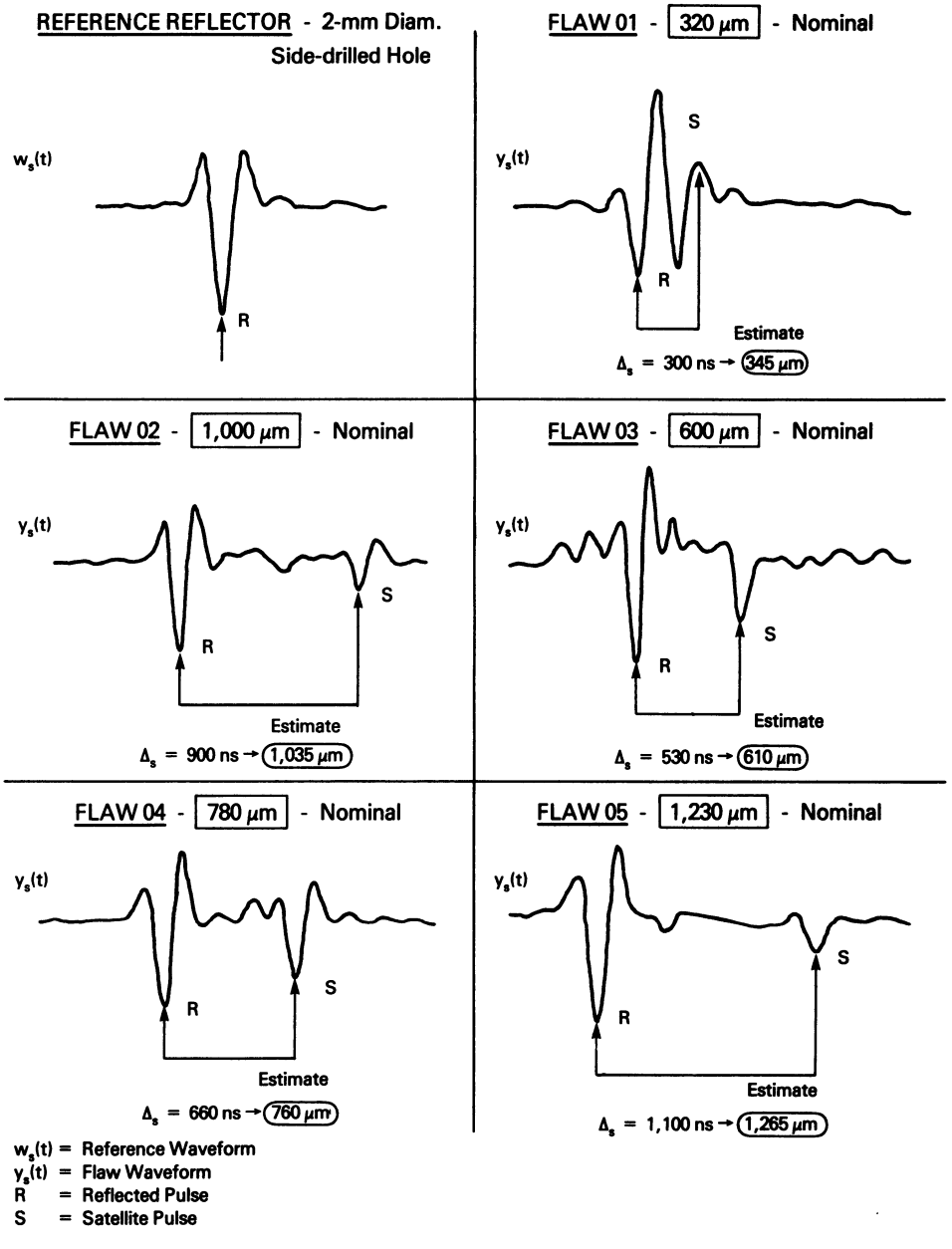

Fig. 4. Satellite Pulses Produced by Insonifying the Five Test Flaws with 7-MHz Shear Waves.

Table 1. Initial Size Estimates Obtained for the Five Test Flaws with High-Frequency Shear Waves

Flaw	Nominal Diameter (μm)	SPOT Diameter Estimate (μm) 6.7 MHz(1)	6.9 MHz(2)	Average
01	320	391	345*	366
			362	
02	1,000	995	1,035*	1,026
		1,035	1,093	
		1,035	960	
03	600	610	719	696
		696	610*	
		771	719	
04	780	719	760*	751
		753	771	
		713	788	
05	1,230	1,443	1,489	1,408
		1,432	1,409	
			1,265*	

(1) 60-Degree Shear Waves
(2) 45-Degree Shear Waves
* Flaw Waveform Included in Figure 4

Table 2. Selection of Transducers for Sizing Voids in Ti-6-4 by the Born Inversion Technique

Flaw	Nominal Diameter d_s (μm)	Optimum Frequency f_o (MHz)	Center Frequencies of Most Appropriate Transducers (MHz)
01	366	5.3	4.1, 9.2
02	1,026	1.9	1.9
03	696	2.8	1.9, 4.1
04	751	2.6	1.9, 4.1
05	1,408	1.4	1.9

transducers. The Born-diameter estimate for this flaw is marginal (see Table 3). For Flaw 05, the optimum frequency could not be bracketed by the available transducers, and the sizing error is significant. For the remaining three flaws, the optimum frequency could be bracketed with the available transducers, but the sizing errors appear to be no better than marginal.

Table 3. Born-Diameter Estimates Obtained for the Five Test Flaws with Moderate-Frequency Longitudinal Waves

Flaw	Nominal Diameter (μm)	BORN Diameter Estimate (μm)			
		1.9 MHz	4.1 MHz	9.2 MHz	10.8 MHz
01	320	---	<446	>290	---
02	1,000	811	---	---	---
03	600	<762	>513	---	---
04	780	<798	>522	---	---
05	1,230	>825	---	---	---

CONCLUSIONS

The preliminary conclusions of the blind tests performed to date are:

- High-frequency shear-wave measurements yield good initial estimates of void size d_s.
- The Born inverse-scattering algorithm yields flaw-size estimates with acceptable inaccuracy, provided that the center frequency of the longitudinal-wave transducer is selected in accordance with the relation $f_o = 1{,}950/d_s$.

REFERENCES

1. Moyzis, J. A. and Forney, D. M., "Increased Reliability - A Critical NDE Research Goal," in Review of Progress in Quantitative Nondestructive Evaluation, Volume 1, 7-11, Plenum Press, New York, 1982.

2. Thompson, R. B. and Gray, T. A., "Range of Applicability of Inversion Algorithms," in Review of Progress in Quantitative Nondestructive Evaluation, Volume 1, 233-249, Plenum Press, New York, 1982.

3. Addison, R. C.; Elsley, R. K.; and Martin, J. F., "Test Bed for Quantitative NDE - Inversion Results," in Review of Progress in Quantitative Nondestructive Evaluation, Volume 1, 251-261, Plenum Press, New York, 1982.

4. Rose, J. H.; Thompson, D. O.; and Thompson, R. B., Subcontract Proposal to Southwest Research Institute for a High Reliability Quantitative Flaw Characterization Module, Ames Laboratory, Iowa State University, March 1981.

5. Request for Proposal No. F33615-81-R-5066, "Exploratory Development for a High Reliability Quantitative Flaw Characterization Module," issued by the Air Force Systems Command, Wright-Patterson Air Force Base, February 1981.

6. Freedman, A., "The High-Frequency Echo Structure of Some Simple Body Shapes," Acustica, Volume 12, 61-70, February 1962.

7. Franz, W. and Deppermann, K., "Theorie der Beugung am Zylinder unter Berücksichtigung der Kriechwellen," Annalen der Physik, Series 6, Volume 10, 361-373, June 1952.

8. Gruber, G. J., "Defect Identification and Sizing by the Ultrasonic Satellite-Pulse (Observation) Technique," Journal of Nondestructive Evaluation, Volume 1, 263-276, December 1980.

9. Harbold, M. L. and Steinberg, B. N., "Direct Experimental Verification of Creeping Waves," Journal of the Acoustical Society of America, Volume 45, 592-603, March 1969.

10. Shambaugh, R. L., Subcontract Proposal to Southwest Research Institute for Quantitative Flaw Characterization Test Specimen Preparation and Initial Flaw Characterization, Pratt & Whitney Aircraft Group, April 1981.

11. Personal Communication with Dr. Thomas J. Moran, Air Force Project Manager, on August 9, 1983.

DISCUSSION

M.J. Buckley (Rockwell International Science Center): I can't help but wonder about the bandwidth of the transducers which you were using. Couldn't you use any wide bandwidth tranducer?

G.J. Gruber: These are as wide band as you can get. These are the transducers that you use and Ames Lab used. These were just the transducers. You could see perhaps from those time domain pictures that the same transducers were used to get those wave-

forms that went into the Born, that went into the S.P.O.T., and some of them were no more that two or three half cycles long. These are just about the best we can have so they were as good as we can make them.

M.J. Buckley: Then I'm surprised you were that dependent on the particular sound frequency.

G.J. Gruber: Yes.

M.J. Buckley: I can't understand that.

G.J. Gruber: The results that we obtained in the Europe Science Center in December and the ones from Ames in June showed the same wide spread.

J.M. Richardson (Rockwell International Science Center): I want to comment that we tried a technique in another context for trying to find the best frequency window for determining properties. We used the technique which was based upon the assumption that there was a model error that increased with frequency that we determined in an adaptive estimation. It automatically provided a window that was good for that particular case without knowing what the case is.

G.J. Gruber: I submit to you there is no simple way of telling what the transducer center frequency should be other than looking at the waveform and look how long these pulses appear to last. You get that on the spot. Your look at it.

J.M. Richardson: This is an automated version.

G.J. Gruber: You can do that automatically, too.